Characterization of cells from patient-derived fibrovascular membranes in proliferative diabetic retinopathy

The Harvard community has made this article openly available. Please share how this access benefits you. Your story matters

Citation	Kim, L. A., L. L. Wong, D. S. Amarnani, A. A. Bigger-Allen, Y. Hu, C. K. Marko, D. Eliott, et al. 2015. "Characterization of cells from patient-derived fibrovascular membranes in proliferative diabetic retinopathy." Molecular Vision 21 (1): 673-687.
Citable link	http://nrs.harvard.edu/urn-3:HUL.InstRepos:17295522
Terms of Use	This article was downloaded from Harvard University's DASH repository, and is made available under the terms and conditions applicable to Other Posted Material, as set forth at http://nrs.harvard.edu/urn-3:HUL.InstRepos:dash.current.terms-of-use#LAA

Characterization of cells from patient-derived fibrovascular membranes in proliferative diabetic retinopathy

Leo A. Kim,[1,2] Lindsay L. Wong,[1] Dhanesh S. Amarnani,[1] Alexander A. Bigger-Allen,[1] Yang Hu,[1] Christina K. Marko,[1] Dean Eliott,[2] Vinay A. Shah,[3] Declan McGuone,[4] Anat O. Stemmer-Rachamimov,[4] Xiaowu Gai,[5] Patricia A. D'Amore,[1,6] Joseph F. Arboleda-Velasquez[1]

[1]Schepens Eye Research Institute/Massachusetts Eye and Ear, Department of Ophthalmology, Harvard Medical School, Boston, MA; [2]Retina Service, Massachusetts Eye and Ear Infirmary, Department of Ophthalmology, Harvard Medical School, Boston, MA; [3]Dean McGee Eye Institute, University of Oklahoma Health Sciences Center, Oklahoma City, OK; [4]C.S. Kubik Laboratory for Neuropathology, Massachusetts General Hospital, Boston, MA; [5]Ocular Genomics Institute, Massachusetts Eye and Ear Infirmary, Harvard Medical School, Boston, MA; [6]Department of Pathology, Harvard Medical School, Boston, MA

Purpose: Epiretinal fibrovascular membranes (FVMs) are a hallmark of proliferative diabetic retinopathy (PDR). Surgical removal of FVMs is often indicated to treat tractional retinal detachment. This potentially informative pathological tissue is usually disposed of after surgery without further examination. We developed a method for isolating and characterizing cells derived from FVMs and correlated their expression of specific markers in culture with that in tissue.
Methods: FVMs were obtained from 11 patients with PDR during diabetic vitrectomy surgery and were analyzed with electron microscopy (EM), comparative genomic hybridization (CGH), immunohistochemistry, and/or digested with collagenase II for cell isolation and culture. Antibody arrays and enzyme-linked immunosorbent assay (ELISA) were used to profile secreted angiogenesis-related proteins in cell culture supernatants.
Results: EM analysis of the FVMs showed abnormal vessels composed of endothelial cells with large nuclei and plasma membrane infoldings, loosely attached perivascular cells, and stromal cells. The cellular constituents of the FVMs lacked major chromosomal aberrations as shown with CGH. Cells derived from FVMs (C-FVMs) could be isolated and maintained in culture. The C-FVMs retained the expression of markers of cell identity in primary culture, which define specific cell populations including CD31-positive, alpha-smooth muscle actin-positive (SMA), and glial fibrillary acidic protein-positive (GFAP) cells. In primary culture, secretion of angiopoietin-1 and thrombospondin-1 was significantly decreased in culture conditions that resemble a diabetic environment in SMA-positive C-FVMs compared to human retinal pericytes derived from a non-diabetic donor.
Conclusions: C-FVMs obtained from individuals with PDR can be isolated, cultured, and profiled in vitro and may constitute a unique resource for the discovery of cell signaling mechanisms underlying PDR that extends beyond current animal and cell culture models.

Proliferative diabetic retinopathy (PDR), a condition characterized by aberrant angiogenesis in the eye, is among the most common and devastating complications of diabetes mellitus and the most frequent cause of blindness in working-age adults in the United States [1-3]. The aberrant vessels in PDR often grow into the vitreous, are leaky, prone to hemorrhage, and can lead to the formation of epiretinal fibrovascular membranes (FVMs) and subsequent tractional or combined tractional and rhegmatogenous retinal detachment, for which surgery is indicated to avoid permanent vision loss [4,5]. Substantial evidence indicates that vascular endothelial growth factor (VEGF) induction plays a crucial role in PDR [6-9]. However, anti-VEGF therapy is rarely used in PDR because this therapy may trigger hemorrhage and retinal detachment [10-14]. Other treatments for PDR include

pan-retinal photocoagulation and surgical removal of the FVMs, though these treatments are not without complications. Pan-retinal photocoagulation may lead to peripheral vision loss, and additional surgical procedures involve high risk in patients with advanced diabetes [15].

A significant barrier for progress in the field is that animal models of diabetes do not develop PDR [16-19]. The available animal models mostly reproduce early-stage DR pathological features including pericyte loss, acellular capillaries, and microaneurysms [20-24]. Thus, PDR pathobiology is usually studied using surrogate models such as oxygen-induced retinopathy and choroidal neovascularization [25-28]. Moreover, currently available in vitro models involve short-term culture of vascular cells under high-glucose conditions that only partially reproduce the diabetic milieu [29]. As these cultures are often derived from non-diabetic donors, the cultures also lack environmental and genetic factors that could be important for the disease. Specifically, cells

Correspondence to: Joseph F. Arboleda-Velasquez, 20 Staniford Street, Boston, MA 02114, Phone: (617) 912-2517; FAX: (617) 912-0128; email: joseph_arboleda@meei.harvard.edu

from diabetic sources have been shown to have "metabolic memory," implicating potential epigenetic changes from continual exposure to a high-glucose environment [30,31]. To address the need for new experimental platforms that allow for the discovery of novel cell signaling mechanisms linked to PDR, we developed a methodology for isolation and culture of cells from patient-derived FVMs.

Recently, a population of cells negative for endothelial cell markers (CD31 and VEGFR2) and partially positive for hematopoietic (CD34, CD47) and mesenchymal stem cell markers (CD73, CD90/Thy-1, and PDGFR-β) was cultured ex vivo from epiretinal membranes from patients and compared to RPE cells [32]. In this study, we report on the evaluation of FVM morphology, subsequent isolation, characterization, and primary culture of CD31-positive and alpha-smooth muscle actin-positive cells from FVMs obtained directly from patients undergoing surgery for PDR.

METHODS

Study population: Eleven patients were recruited from Massachusetts Eye and Ear and Dean McGee Eye Institute. Seven patients had type 1 diabetes mellitus, while four patients had type 2 diabetes mellitus. All patients were medically cleared for surgery. Six subjects were male, and five subjects were female. The mean age was 41.7 years old, with ages ranging from 28 to 59 years old. This study was performed at the Schepens Eye Research Institute/ Massachusetts Eye and Ear. Research protocols were approved by the Institutional Review Board at Massachusetts Eye and Ear for the collection of surgical specimens and for the retrospective analysis of the clinical data. Similarly, Institutional Review Board approval was also obtained from the Dean McGee Eye Institute at the University of Oklahoma Medical Center to collect additional surgical and blood specimens. All research protocols adhered to the tenets of the Declaration of Helsinki [33], and each patient signed a consent form and Health Information Portability and Accountability Act (HIPAA) authorization before participation within the study. All research protocols adhere to the ARVO statement on human subjects and to the tenets of the Declaration of Helsinki [33]. Each patient signed a consent form and Health Information Portability and Accountability Act (HIPAA) authorization before participation within the study.

Patients were selected and included in the study if they presented with active fibrovascular proliferation due to PDR with retinal detachment or vitreous hemorrhage not amenable to observation or further treatment with pan-retinal photocoagulation. Patients were excluded from the study if they were under the age of 18, pregnant, not medically stable for surgery, or had a history of previous penetrating eye trauma. The patients' records were obtained and reviewed to record demographic and clinical data. Fundus photography was performed with Optos wide field imaging (Optos, Scotland, UK) where indicated and possible. Blood was drawn from all study participants through venipuncture for comparative genomic hybridization. Blood was drawn from subject with standard methods for venipuncture into EDTA collection tubes, and immediately stored at 4 °C. Genomic DNA was isolated from blood using a Qiagen DNeasy Blood and Tissue Kit (Qiagen, Valencia, CA). Blood samples from the University of Oklahoma were delivered at room temperature using overnight mail.

All patients underwent standard 23-gauge three-port pars plana vitrectomy using a combination of delamination and segmentation techniques with intraocular forceps, scissors, and a vitrector. Extensive panretinal photocoagulation using endolaser was performed on all patients. Retinal tamponade was performed with non-expansile C3F8 gas or silicone oil. Control retina samples were obtained from cadaver eyes through an approved Institutional Review Board protocol from Massachusetts General Hospital.

Processing of surgically-removed FVMs: Immediately after surgery, the FVMs were placed in ice-cold calcium-free and magnesium-free Hank's balanced salt solution for transportation. Membranes were divided into pieces and processed for electron microscopy, immunohistochemistry, or cell culture. The size of the FVM tissue recovered during surgery was a limiting factor that determine the number of procedures and studies conducted in each sample. The FVM samples obtained from the University of Oklahoma were shipped on dry ice and used for genetic studies only.

Immunohistochemistry: FVMs and samples of control retinas were fixed in 10% formalin in Dulbecco's PBS (1X; 137 mM NaCl, 2.7 mM KCl, 8 mM Na_2PO_4, 1.47 mM KH_2PO_4, pH 7.4) overnight at room temperature and stored in PBS at 4 °C until paraffin embedding. Serial sections (6 μm) were cut, deparaffinized in 100% xylene, rehydrated in a series of ethanol, and washed in PBS. Sections were processed for immunohistochemistry using the following antibodies: CD31 (1:50; Dako, Carpinteria, CA), alpha-smooth muscle actin (SMA, 1:50; Dako), glial fibrillary acidic protein (GFAP, 1:500; Dako), retinal pigment epithelium-specific protein 65 (RPE65, 1:250; Chemicon, Billerica, MA), bestrophin-1 (BEST-1, 1:150; Abcam, Cambridge, MA), and Ki67 (1:50; Novus Biologicals, Littleton, CO). Heat-induced epitope retrieval, as recommended by the manufacturer, was performed in either boiling citrate buffer (pH 6) for RPE65, BEST-1, and Ki67 or boiling Tris-EDTA buffer (pH 9) for CD31 and SMA; proteinase

K was used as the antigen retrieval method for GFAP. The slides were then incubated in 3% H_2O_2 in methanol to block endogenous peroxidases and then blocked in protein blocking solution and incubated in primary antibody overnight at 4 °C. The following day, sections were incubated in a biotinylated secondary antibody for 1 h followed by alkaline phosphatase-conjugated avidin (Vectastain ABC-AP Universal Kit; Vector Laboratories, Burlingame, CA) for 30 min and then visualized with the Vector Red chromogenic substrate kit (SK-5100; Vector Laboratories). For the Ki67 samples, tyramide signal amplification (TSA, PerkinElmer, Waltham, MA) was performed following incubation in biotinylated secondary antibody, and the Vector Red chromogenic substrate was added. Finally, the slides were counterstained with Gill no. 3 hematoxylin (Sigma-Aldrich, St. Louis, MO), and coverslips were mounted with Permount medium (Thermo Fisher Scientific, Waltham, MA) before imaging using an Axioskop 2 MOT Plus microscope (Carl Zeiss Inc., Thornwood, NY).

Cellularity and staining for CD31, SMA, GFAP, RPE65, BEST-1, and Ki67 within the FVMs were analyzed by quantifying the number of nuclei and the number of marker-positive cells using ImageJ (Version 1.47; NIH, Bethesda, MD). Since the number of nuclei was quantified in sections for each marker, the number of nuclei is presented as the average for each individual case. To standardize for the size differences in FVMs obtained from different patients, ImageJ was used to measure the area of each FVM on the same section for which counts of marker-positive cells were performed. Results are expressed as the number of CD31, SMA, GFAP, RPE65, and BEST-1-positive cells per 10 μm^2. Ki67 data are expressed as a percentage of the positive cells to match the format of the data obtained from the Muse flow cytometry analyzer.

Cell isolation and culture of C-FVMs: With the aid of a dissecting microscope, FVMs were transferred into 500 µl PBS buffer containing 1021 Unit/ml collagenase II (Worthington, Lakewood, NY) and 0.25% bovine calf serum (Hyclone, Logan, UT) and incubated at 37 °C for 60 min. Subsequently, the C-FVMs were washed once in Dulbecco's modified Eagle's medium (DMEM; Lonza, Walkersville, MD) containing 1% L-glutamine, 5% bovine calf serum (Hyclone), 2.5% weight/vol nystatin, 100 U/ml penicillin G, and 100 mg/ml streptomycin by brief centrifugation. FVM cells were resuspended in 250 µl of FVM medium that consisted of endothelial basal medium 2 (EBM2; Lonza) supplemented with the endothelial cell growth media (EGM-2) Bullet Kit (Lonza), 100 U/ml penicillin, 100 mg/ml of streptomycin (Lonza), 2 mM of L-glutamine (Lonza), 12% fetal bovine serum (FBS; final concentration obtained by adding the serum aliquot included with the EGM-2 Bullet

Kit and additional fetal bovine serum; Atlanta Biologicals, Flowery Branch, GA), and 15 mM D-glucose (final concentration obtained by supplementing the 5 mM D-glucose already present in the EBM2 with additional D-glucose purchased from Sigma) and seeded onto culture plates coated with 0.2% gelatin in PBS.

Isolation of CD31-positive cells: Single-cell suspensions of the C-FVMs prepared as described earlier were incubated with 20 µl of CD31 Dynabeads (Invitrogen Dynal AS, Oslo, Norway) in PBS containing 2% FBS, mixed gently, and placed on a shaker (Barnstead/Thermolyne, Dubuque, IA) at 4 °C for 15 min. CD31-positive cells were isolated by using the beads via a magnetic rack and washed twice with PBS containing 2% FBS. The CD31-positive cells were resuspended in 250 µl culture medium that consisted of FVM medium supplemented with VEGF to a final concentration of 6 ng/ml and seeded onto a culture plate previously coated with 1% laminin and 1% collagen Type I in PBS.

Immunofluorescence: C-FVMs were seeded on a four-well Chamber Slide System (Thermo Fisher Scientific). Cells were fixed with 4% paraformaldehyde for 10 min, permeabilized with 0.25% Triton X-100 in PBS for 5 min, and blocked (10% goat serum in PBS) for 1 h. To identify smooth muscle cells and myofibroblasts, cultures were incubated with a fluorescein isothiocyanate (FITC)-conjugated monoclonal anti-SMA primary antibody (1:150; Sigma). To label astrocytes and glial cells, cells were incubated with a rabbit polyclonal anti-GFAP primary antibody (1:150; Dako) overnight at 4 °C followed by incubation with goat anti-rabbit Alexa Fluor 488 secondary antibody (1:200; Life Technologies, Carlsbad, CA) for 2 h at room temperature. CD31 staining was performed using a similar procedure with the CD31 primary antibody (1:50; Dako, Carpinteria, CA) and anti-mouse Alexa Fluor 647 secondary antibody (1:200; Life Technologies, Carlsbad, CA). Isolectin B4 staining was performed using isolectin B4 primary antibody directly conjugated to Alexa Fluor 648 (1:100, Invitrogen, Carlsbad, CA). Coverslips were mounted onto the chamber slides using a Prolong Gold antifade reagent with 4',6-diamidino-2-phenylindole (DAPI; Life Technologies). Images were obtained using a Zeiss Axioskop 2 MOT Plus microscope (Carl Zeiss Inc.).

Muse flow cytometry analysis: Cell proliferation of the C-FVMs from clinical cases 3 and 5 were determined using the Muse Ki67 Proliferation Kit (EMD Millipore, Hayward, CA). Passage 4–6 cells were plated in a 12-well plate and treated with a standard growth medium consisting of FVM medium or the same media that did not contain FBS or the EGM Bullet Kit (growth factor deprivation medium). Cells were harvested using trypsin and resuspended in PBS at a

cellular concentration of 5.0×10^5 cells/ml. The cell suspensions were washed, pelleted, resuspended in 50 µl of fixative solution, and incubated at room temperature for 15 min. The samples were then washed and incubated in permeabilization buffer for 15 min. Following the wash in PBS, the pellets were resuspended in 50 µl of buffer solution and were incubated in 10 µl of Muse Hu IgG1-PE or Muse Hu Ki67-PE for 30 min at room temperature and protected from light exposure. After 150 µl of Muse assay buffer was added to each sample and mixed thoroughly, the samples were run on the Muse cell analyzer to separate and determine the percentages of Ki67-positive and Ki67-negative populations.

Angiogenesis antibody array: Passage 4–6 cells were cultured for 9 days in growth factor deprivation medium; 1.5 ml of supernatant from the clinical case 3 C-FVM was collected, and protein secretion was analyzed using the Human Angiogenesis Antibody Array Kit (R&D Systems, Minneapolis, MN). The membrane, containing antibodies for 55 proteins related to angiogenesis, was immersed in 1.5 ml of 2:1 supernatant and array buffer (included in the kit), as well as 15 µl of reconstituted antibody cocktail. Following incubation in blocking buffer for 1 h, the membrane was incubated overnight on a rocking platform at 4 °C, washed three times for 10 min, submerged in 2 ml of diluted streptavidin-horseradish peroxidase (HRP) in array buffer, and incubated for 30 min at room temperature. Following a rinse in the wash buffer, the membrane was coated with 1 ml of the chemireagent mix. Kodak BioMax light film (Cat. No. 1788207, Eastman Kodak Company, Rochester, NY) was placed over the membrane and allowed to sit in the dark for 30 min. The film was then processed and developed using a Kodak M35A film processor (Eastman Kodak Company) and scanned with an Epson Perfection V500 (Long Beach, CA) photo scanner.

ELISA measurement of angiopoietin-1, thrombospondin-1, PEDF, and endothelin-1: Quantitative comparison of angiopoietin-1 (Ang-1; R&D Systems), thrombospondin-1 (Tsp-1; R&D Systems), pigment epithelium-derived factor (PEDF; Millipore, Temecula, CA), and endothelin-1 (ET-1; R&D Systems) protein in HRP control cells and C-FVMs cultured in different glucose concentrations and osmolarity was determined using enzyme-linked immunosorbent assay (ELISA). Cell-free supernatants from HRP control cells and the C-FVMs from clinical case 3 were collected 9 days after treatment with 5 mM, 15 mM, and 30 mM D-glucose and 5 mM D-glucose plus 25 mM L-glucose (osmotic control).

Student *t* tests were used to evaluate differences in the Ang-1, Tsp-1, PEDF, and ET-1 protein levels under different glucose and osmolar conditions, and compared to the 5 mM D-glucose group. $p < 0.05$ was considered statistically significant. All values in the ELISA results are expressed as mean ± standard deviation.

RESULTS

Clinical demographics and case report: Eleven eyes from 11 patients were enrolled in the study, and the demographic and clinical information for each patient is listed in Appendix 1. Clinical case 3 illustrates a typical case of a woman aged 29 years with type 1 diabetes with combined tractional and rhegmatogenous retinal detachment of the left eye (Figure 1A). Visual acuity was light perception in the right eye and 20/200 in the left eye. The patient's ocular history was significant for a previous macula involving tractional retinal detachment in the right eye that underwent vitrectomy surgery and the placement of silicone oil. The patient underwent vitrectomy with segmentation and delamination of FVM in the left eye with placement of non-expansile C3F8 gas. At post-operative month 3 (POM3), the patient developed a cataract in the left eye, and visual acuity was 20/100. At post-operative month 5 (POM5), the patient underwent cataract surgery, and the retina remained attached with visual acuity of 20/25 (Figure 1B). The FVM was delaminated and visualized under light microscopy (Figure 1C) and grossly appeared to be a combined neovascular-fibrotic membrane, as blood vessels were clearly visualized within the tissue (Figure 1C, inset). The C-FVMs were isolated as described in the Methods section, and in culture formed a monolayer of cells with fibroblastic and stellate morphology (Figure 1D).

Ultrastructural examination of FVMs: Consistent with previous reports, electron micrographic examination of the FVM tissue from clinical case 1 (Appendix 2, A,B) showed numerous blood vessels and vessel-like structures, large areas of fibrosis, and numerous scattered stromal cells, some with no clear association to vascular structures [34]. There were different types of vascular abnormalities (Appendix 2, C), including disorganized microvessels and irregular perivascular cell investment (Appendix 2, D). Many of the vascular cells had large nuclei and plasma membrane infoldings. Some of the perivascular cells appeared to have swollen mitochondria (Appendix 2, C). These morphological features are reminiscent of vascular cells from tumors, which have been shown to carry large chromosomal and centrosomal aberrations, an indication of genomic instability [35-37].

Genomic integrity of FVMs: In light of the ultrastructural abnormalities previously reported [34] and currently observed (Appendix 2) in cells from FVMs, we determined whether cells from FVMs carried genomic abnormalities characteristic of other proliferative conditions [36]. For this purpose, we compared DNA extracted from FVMs with DNA

extracted from the blood of the same donor using comparative genomic hybridization (CGH) analysis. This analysis, which was conducted on paired samples from five unrelated donors, indicated that cells from FVMs lack major somatic chromosomal abnormalities or aneuploidies (clinical cases 7–11).

We observed that different segmentation algorithms identified potential focal copy number variations (8.5 Kb to 3.7 Mb, Appendix 3). The significance of this finding remains to be determined, although we also noted that the DNA amplification step that was required to conduct this analysis using limiting amounts of DNA from the FVM (approximately 50–70 ng, see Methods) is known to generate artifacts, especially for genes that contain repetitive sequences [38–40]. To address this issue, we conducted a single nucleotide polymorphism (SNP) array in one additional donor (clinical case 3) from which sufficient genomic DNA from the FVM was obtained for analysis, and thus, DNA amplification was not required. Again, large chromosomal aberrations were absent. This result differs from previous reports of large chromosomal aberrations and aneuploidies in vascular cells from tumors [35-37], another condition also characterized by aberrant neovascularization.

Immunohistological characterization of FVMs: To evaluate the identity of the cellular components, we examined FVMs from clinical cases 2–6 versus a control retina using immunohistochemistry. Staining of the control retina (Figure 2A–E) revealed expected staining of blood vessels with antisera against CD31 in endothelial cells and labeling for SMA in mural cells. Staining of glial cells within the nerve fiber layer for GFAP can be seen as the processes surrounding the blood vessels. Finally, RPE65 and BEST-1 staining localized to the RPE.

The staining patterns among the various FVMs were variable (Figure 2). Table 1 illustrates the number of nuclei per surface area of FVM for the total number of cells that were labeled for CD31, SMA, GFAP, and BEST-1 antibodies. No FVMs stained positively for RPE65. Cases 3 and 5 had the highest number of nuclei (188.17 and 151.62 nuclei/10 μm^2, respectively). Further, these two cases also had the most CD31-positive (21.22 and 21.20 nuclei/10 μm^2, respectively), SMA-positive (168.86 and 105.58 nuclei/10 μm^2 respectively), and BEST-1-positive (87.99 and 50.81 nuclei/10 μm^2, respectively) cells. In contrast, cases 2 and 6 had moderate numbers of CD31-positive cells (7.78 and 12.83 nuclei/10 μm^2, respectively), and case 2 contained higher levels of SMA-positive
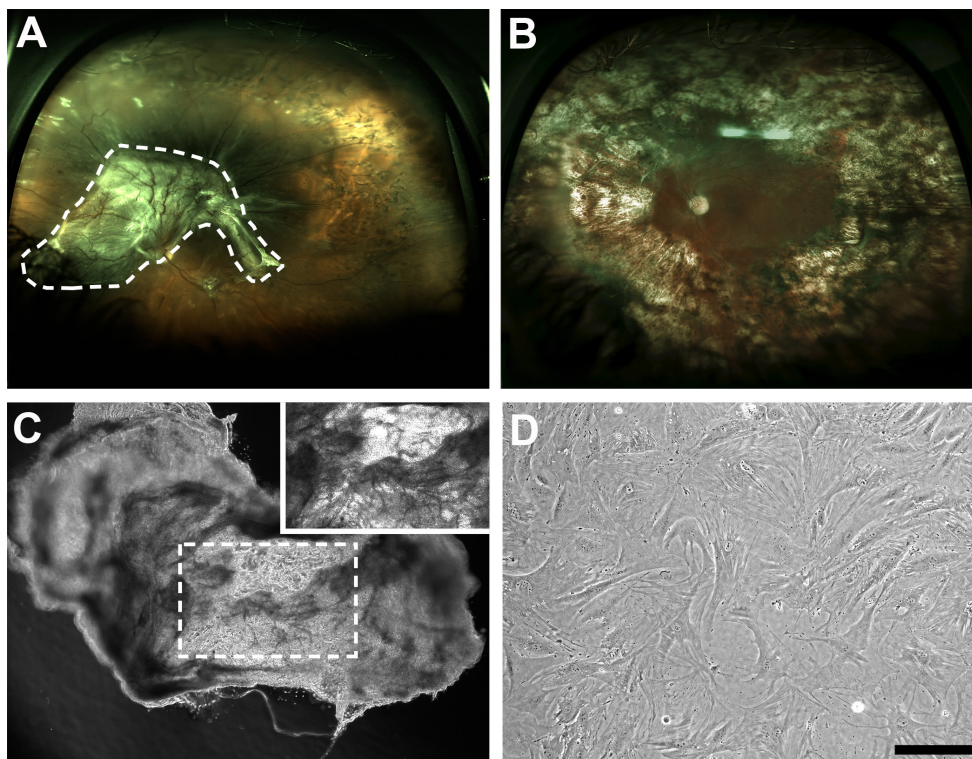

Figure 1. Clinical case 3 representing combined tractional and rhegmatogenous retinal detachment with resection of FVM and growth of C-FVM. Pre-operative fundus photograph of the left eye reveals combined tractional and rhegmatogenous retinal detachment of the left eye with 20/200 vision (**A**). FVM (outlined by dotted white line) involves the macula and reveals fibrous tissue with aberrant blood vessels. Post-operative fundus photograph five months post vitrectomy and one month after cataract surgery demonstrates re-attached retina with 20/25 vision (**B**). Bright field microscopy of surgically resected FVM shows fibrous tissues and blood vessels (**C**, inset). Bright field microscopy of cells derived from FVM reveals a morphologically heterogeneous mixture of fibroblastic and stellate cells (**D**). Scale bar = 100 μm.
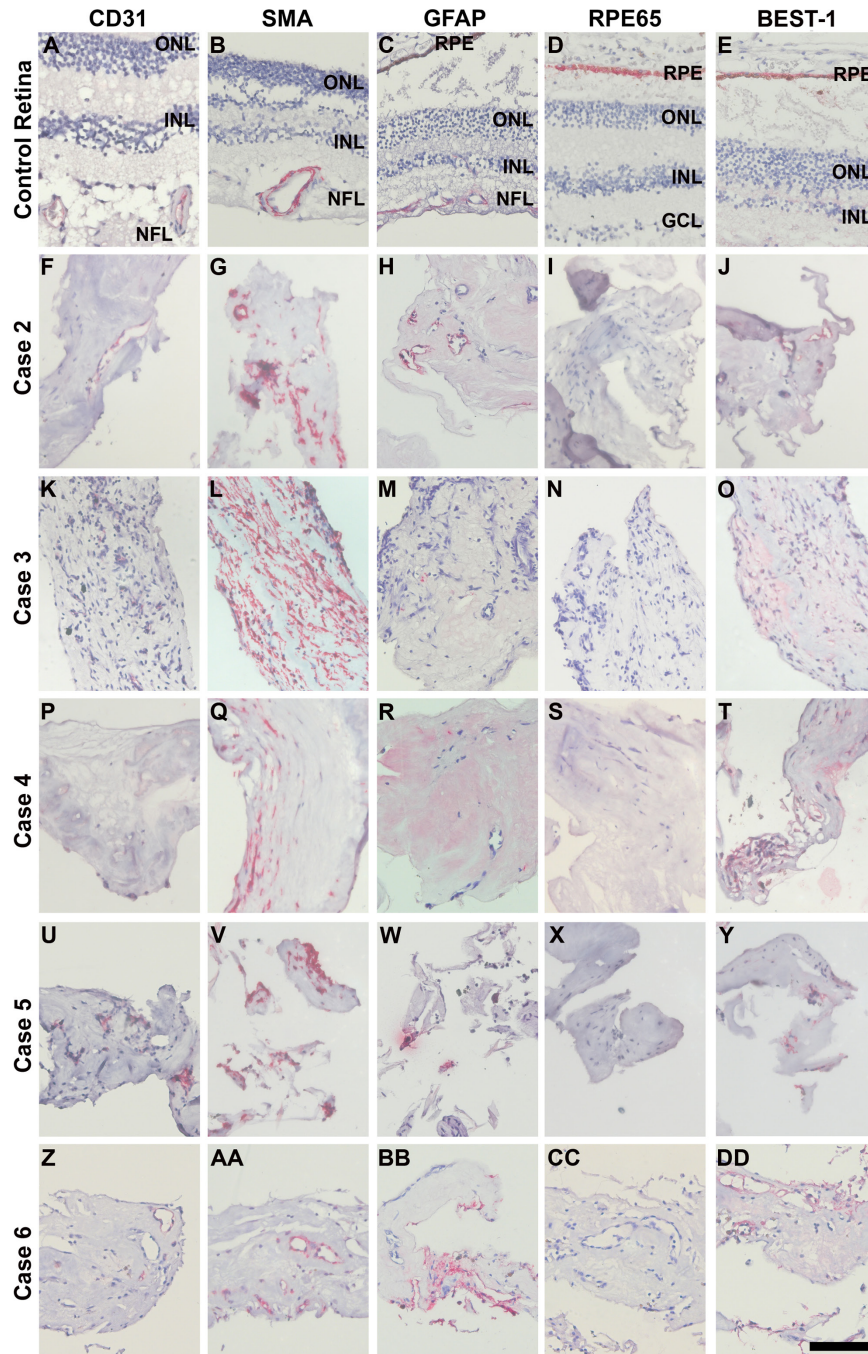
Figure 2. Histopathological characterization of FVM tissue from patients with severe PDR. Light micrographs of the control retina (**A–E**) and fibrovascular membranes (FVMs) from five different cases (**F–DD**) processed for immunohistochemistry using primary antibodies against CD 31 (**A, F, K, P, U, Z**), smooth muscle actin (SMA, **B, G, L, Q, V, AA**), glial fibrillary acidic protein (GFAP, **C, H, M, R, W, BB**), retinal pigment epithelium-specific protein 65 (RPE65, **D, I, N, S, X, CC**), and bestrophin-1 (BEST-1, **E, J, O, T, Y, DD**; all in *red*) and counterstained with hematoxylin (*blue*). In the control retina, faint CD31 staining of endothelial cells is observed (**A**), SMA localization is restricted to vessels (**B**), GFAP staining localizes to cells surrounding the blood vessels within the nerve fiber layer (*NFL*, **C**), and RPE65 and BEST-1 localize to the RPE cells (**D, E**). For FVMs derived from different patients, however, there was notable variability in the localization patterns and the number of positive cells for the different markers. All FVMs have CD31-positive cells, which are perivascular (**F, K, P, U, Z**). SMA-positive cells were also detected in all FVMs; some SMA staining was localized predominately to cells surrounding the vessels (**G, AA**) whereas other SMA-positive cells appear to be stromal (**L, Q, V**), located throughout the fibrous tissue of the FVM. GFAP-positive cells are also observed in all FVMs; some GFAP-positive cells are seen surrounding vessels (**H, BB**) whereas other GFAP-positive cells are located within the stroma of the FVM (**M, R, W**). Whereas all FVMs are RPE65-negative (**I, N, S, X, CC**), BEST-1 positive cells are distributed throughout the FVM tissue, as well as localized to perivascular cells (**J, O, T, Y, DD**). Scale bar=100 μm.

cells versus case 6 (51.44 and 10.82 nuclei/10 μm², respectively), and fewer GFAP-positive cells (6.93 and 51.58 nuclei/10 μm², respectively). Furthermore, the localization of SMA-positive cells differed between these two cases. In case 2, SMA-positive cells were found surrounding blood vessels as well as the stroma (Figure 2G), whereas in case 6, SMA-positive cells were found exclusively adjacent to blood vessels (Figure 2AA). In addition, the localization of GFAP-positive cells was different between these two cases. In case 2, GFAP-positive cells were localized around blood vessels (Figure 2H), whereas in case 6, GFAP-positive cells were surrounding blood vessels as well as the stroma (Figure 2BB). Cases 2 and 6 contained similar amounts of BEST-1-positive cells (24.3 and 30.43 nuclei/10 μm², respectively) in association with blood vessels (Figure 2J,DD). Case 4 had the fewest CD31-positive cells (1.36 nuclei/10 μm²), a moderate number of SMA-expressing cells (20.26 nuclei/10 μm²), no cells that were positive for GFAP, and the fewest BEST-1 positive cells (10.51 nuclei/10 μm²). These data indicate that quantification and localization of the specific cell markers vary extensively among FVMs removed from patients with PDR.

Isolation, cell culture, and characterization of C-FVMs: Having shown that cells from FVMs are a genetically homogenous population using CGH and that they express specific markers of cell identity, we then established methodologies for isolation and primary culture of the cells. Cells displaying mural cell, fibroblast, or stellate morphology were clearly identified, suggesting the presence of pericytes, myofibroblasts, and glial cell populations (Figure 1D).

To determine whether C-FVMs retained their phenotypes in culture, we conducted immunohistochemistry analyses of tissue and of cells cultured from FVM fragments obtained from the same donor (Figure 3). SMA-positive cells were abundant in the FVM derived from clinical case 3 and were also detected in the C-FVMs derived from the same donor (Figure 3A,C). Other cell populations, including GFAP-positive cells, were also identified in the cell culture (Figure 3B,D). SMA-positive and GFAP-positive cells were identified in cells cultured from the FVM of case 5 (Figure 3E–H), indicating that the C-FVMs retain the expression of some markers expressed by cells in the tissue.

Cell proliferation analysis: FVMs from cases 3 and 5, which appeared to have the highest number of nuclei, gave rise to robust cultures that were expanded and stored. We examined Ki67 staining in FVM fragments from clinical case 3 and 5 and found Ki67-positive cells in both FVMs (Figure 4A,B). Approximately 63% of the cells were Ki67-positive in the FVM from clinical case 3 and approximately 28% of the cells were Ki67-positive in the FVM from clinical case 5. Additionally, we used a microcapillary Muse cell analyzer to examine the Ki67-positive cells in the FVM-derived cultures and also observed a difference in percentage of Ki67-positive cells, as the culture of the cells from case 3 had more proliferating cells (33.94%) in growth-factor rich media compared to the proliferation rate of cells from case 5 (18.40%; Figure 4C,D). In contrast, in growth-factor reduced conditions, cases 3 and 5 had roughly equivalent rates of cell proliferation with 7.43% and 5.94% Ki67-positive cells, respectively (Figure 4E,F). Our finding may indicate that cellular proliferation rates in vitro reflect cellular proliferation in situ with the FVMs themselves.

Isolation of CD31-positive C-FVMs: Isolectin B4 and CD31-positive cells were infrequently identified in the primary cultures (Figure 5A,B). This was unexpected because the CD31-positive cells were clearly identified lining vessels in the FVMs (Figure 5C). However, we reasoned that because the original culture after tissue digestion represented a mix of different cell populations, perhaps other cell populations were inhibiting the growth of the CD31-positive cells and taking over the culture. We have previously shown that coculture of endothelial cells with mural cells leads to the activation of transforming growth factor-β that limits the growth of endothelial cells [41]. To avoid this limitation, CD31-positive cells were isolated using CD31 antibody coated Dynabeads immediately before cell culture. The CD31-positive C-FVMs were maintained in laminin/collagen 1-coated culture dishes in the

Case No.	Avg Nuclei/10 μm²	CD31+/10 μm²	SMA+/10 μm²	GFAP+/10 μm²	BEST-1+/10 μm²
2	69.790	7.782	51.441	6.926	24.303
3	188.171	21.223	168.861	1.591	87.994
4	51.606	1.361	20.263	0	10.507
5	151.615	21.200	105.582	3.665	50.810
6	47.599	12.826	10.822	51.578	30.433

TABLE 1. CHARACTERISTICS OF FVMs REMOVED FROM PATIENTS WITH DIABETES MELLITUS.

BEST=bestrophin-1; CD31=cluster of differentiation 31; FVM=fibrovascular membrane; GFAP=glial fibrillary acidic protein; SMA=smooth muscle actin.
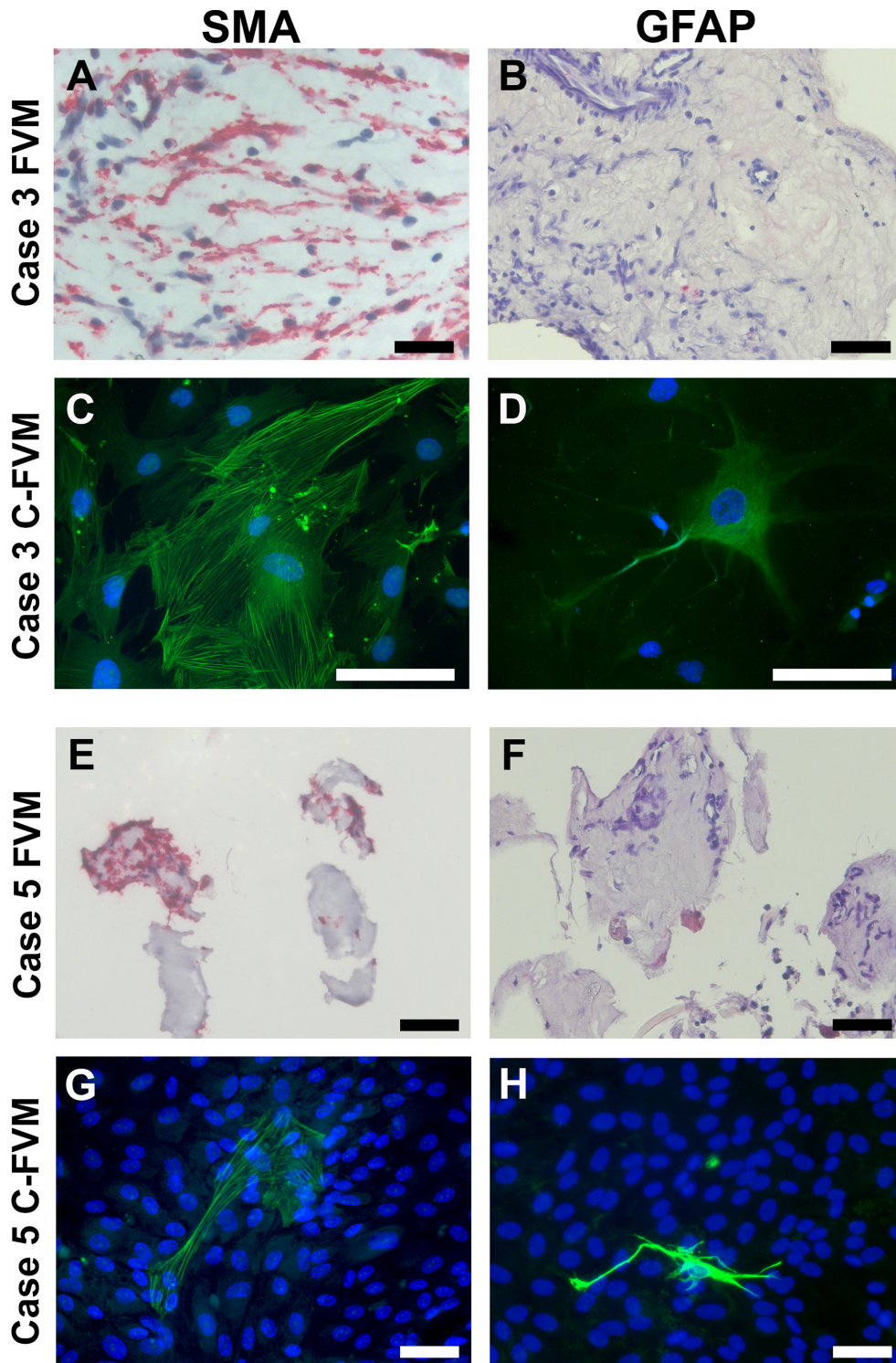
Figure 3. Histopathological characteristics of FVMs are retained in C-FVMs. Fibrovascular membranes (FVMs) from clinical cases 3 and 5 were processed for immunohistochemistry using antibodies against SMA (**A, E**) and GFAP (**B, F**; all in *red*) and counterstained with hematoxylin (*blue*). Immunofluorescence of the C-FVMs shows cells positive for SMA (**C, G**) and GFAP (**D, H**; in *green*), indicating that molecular markers of cell identity are retained in C-FVMs grown in vitro. Nuclei are counterstained with 4',6-diamidino-2-phenylindole (DAPI; *blue*). Scale bar=50 μm.

presence of 6 ng/ml VEGF (Figure 5D). Our data indicate that CD31-positive cells from FVM tissue can be cultured when selected at the time of initial isolation.

Profiling angiogenesis-related factors secreted by C-FVMs: An antibody array targeting 55 proteins was used to examine the angiogenesis-related factors secreted by the SMA-positive/CD31-negative C-FVMs in the primary culture from case 3. Appendix 4 identifies the 55 angiogenesis-related proteins assayed with the human angiogenesis antibody array and gives their coordinates on the membrane. Of the 55 targeted proteins, 11 proteins were detected in the supernatants of cells derived from the case 3 FVM. The C-FVMs expressed angiogenin (ANG), Ang-1, ET-1, insulin-like growth factor binding proteins 2 and 3 (IGFBP-2 and IGPBP-3), monocyte chemoattractant protein-1 (MCP-1), plasminogen activator inhibitor-1 (PAI-1), pentraxin 3 (PTX-3), pigment epithelium-derived factor (PEDF), TIMP metallopeptidase inhibitor 1 (TIMP-1), and Tsp-1 (Figure 6A). To confirm that these secreted proteins are indeed being made by the C-FVMs, we looked at the mRNA expression levels of a subset of these proteins. Quantitative reverse transcription-PCR (RT-qPCR) confirmed the expression of Ang-1, ET-1, PEDF, and Tsp-1 in the cultured SMA-positive/CD31-negative C-FVMs from clinical case 3 (Appendix 5). To examine whether the C-FVMs responded differentially to a diabetic environment, we cultured the SMA-positive/CD31-negative C-FVMs from case 3 in high-glucose or hyperosmolar conditions and measured the levels of secreted factors using ELISA. Since these C-FVMs were SMA-positive, we chose to compare them to primary retinal pericytes derived from a non-diabetic donor, a cell type that also expresses this cell marker [42,43]. High glucose or hyperosmolarity triggered a statistically significant decrease in the secretion of Ang-1 and Tsp-1 (Figure 6B,C) but had no effect on PEDF or ET-1 secretion (Figure 6D,E). In contrast, under similar conditions, SMA-positive human retinal pericytes derived from a non-diabetic donor showed no significant change in the secretion of these factors (Figure 6B-E).
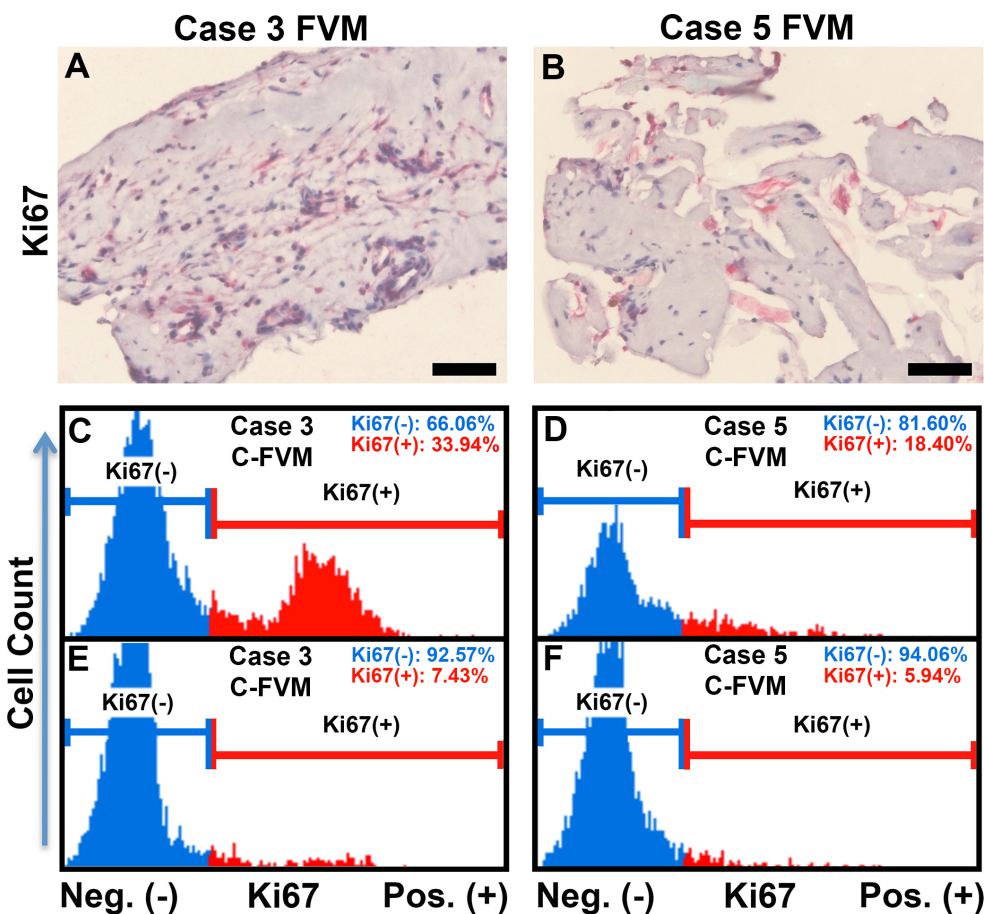

Figure 4. Proliferative activity of C-FVMs varies between different clinical cases. Fibrovascular membranes (FVMs) from clinical cases 3 (**A**) and 5 (**B**) were processed for immunohistochemistry using antibodies against Ki67 (in *red*) and counterstained with hematoxylin (*blue*). C-FVMs from clinical case 3 and clinical case 5 differ in the percentage of cells that are Ki67-negative (66.06% versus 81.60%) and Ki67-positive (33.94% versus 18.40%) when cultured in growth media (**C, D**). The percentage of cells that are Ki67-negative (92.57% versus 94.06%) and Ki67-positive (7.43% versus 5.94%) in C-FVMs from clinical cases 3 and 5 are similar under growth factor-starvation conditions (**E, F**). Scale bar=50 μm.
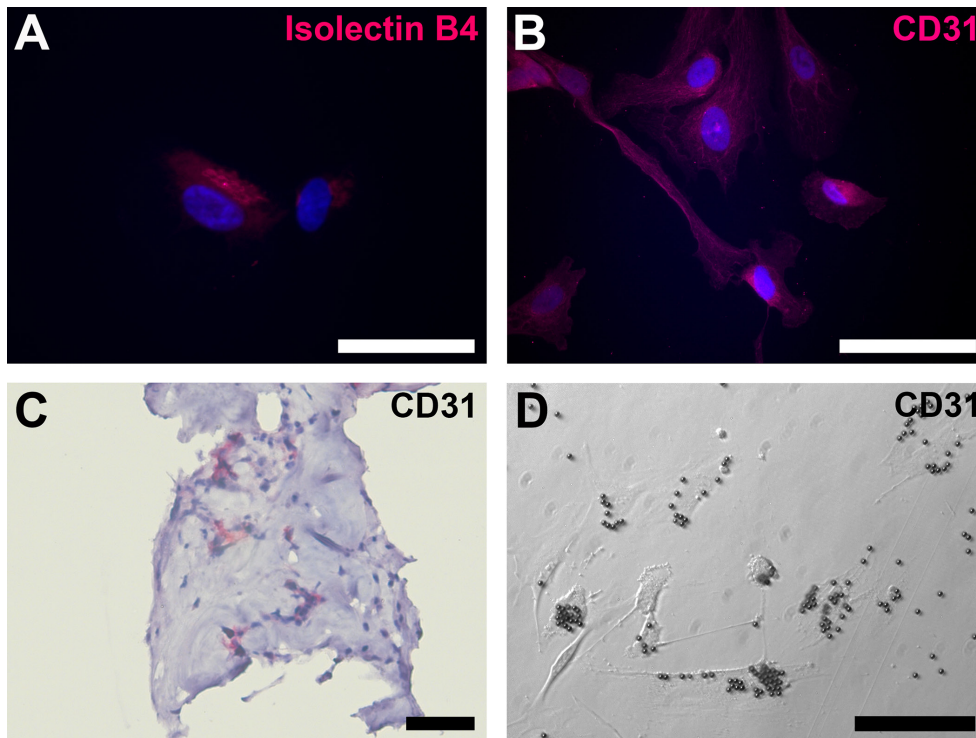
Figure 5. Isolation of CD31-positive cells from C-FVMs. Immunofluorescence localization of isolectin (**A**) and CD31 (**B**) cells from clinical case 4 identifies rare positive cells. Fibrovascular membrane (FVM) from clinical case 5 processed for immunohistochemistry using antibodies against CD31 (*red*) and counterstained with hematoxylin (*blue*; **C**). Light micrographs of C-FVMs from clinical case 5 show isolation of CD31-positive cells, bound to CD31-antibody coated Dynabeads before cell culture (**D**). Scale bar=50 μm.

DISCUSSION

In this work, we report the isolation, culture, and characterization of cells from FVMs or C-FVMs derived from patients with proliferative diabetic retinopathy, the most prevalent cause of vision loss in working-age adults in developed countries [44]. Parallel analyses in tissue and cell culture demonstrate that C-FVMs in primary culture retain at least some cell identity markers found in their tissue of origin, secrete factors relevant to the regulation of angiogenesis, and may respond to high glucose or hyperosmolar conditions differently than cells derived from non-diabetic donors. Because C-FVMs are derived from a relevant pathological tissue and have been exposed to a diabetic environment for the duration of the disease, they may represent a unique tool for elucidating the pathobiological mechanisms that underlie PDR.

We found that SMA-positive C-FVMs expressed several signaling molecules with angiogenic and antiangiogenic properties including ANG, Ang-1, IGFBP-2, IGPBP-3, MCP-1, PAI-1, PTX-3, PEDF, TIMP-1, Tsp-1, and ET-1. These results are consistent with previous reports on the secretion of angiogenesis related factors by cells derived from FVMs [32] and suggest that these cells may be participants, not bystanders, in PDR pathology. In fact, we found that under conditions that mimic a diabetic environment (e.g., high glucose or hyperosmolarity), C-FVMs secrete lower levels of Ang-1 and Tsp-1, factors that are involved in the stabilization and/or inhibition

of angiogenesis [45-47], compared to cells from a non-diabetic donor. These results suggest that the use of C-FVMs for analyzing phenotypic changes induced by diabetes may be more relevant than retinal vascular cells derived from non-diabetic sources, which are the current standard in the field. Whether somatic mutations arising in situ play a role in the proliferative phenotype of cells from FVMs requires further investigation, although our CGH studies indicate that, unlike vascular cells from tumors [35-37], cells from FVMs lack major chromosomal and centrosomal anomalies.

The Ang1-Tie2 system is involved in endothelial-stromal cell interactions and regulates vascular maturation and stability [48,49]. Overexpression of Ang1 has also been found to block the permeability-inducing effects of VEGF in vivo and, thus, has been proposed as a therapeutic option for the treatment of aberrant neovascularization in the eye [46,50]. High levels of Ang1 were found in patients with non-proliferative DR when compared to patients with PDR [51]. Consistent with this observation, C-FVMs cultured in high-glucose or hyperosmolar conditions had reduced Ang1 expression, which may contribute to vascular instability in PDR. Similarly, C-FVMs responded to high glucose or hyperosmolarity by decreasing the expression of Tsp-1, a potent endogenous inhibitor of angiogenesis [45,52]. Loss of Tsp-1 in vitreous samples from diabetic rats has been associated with early retinopathy [5]. Consequently, downregulation of
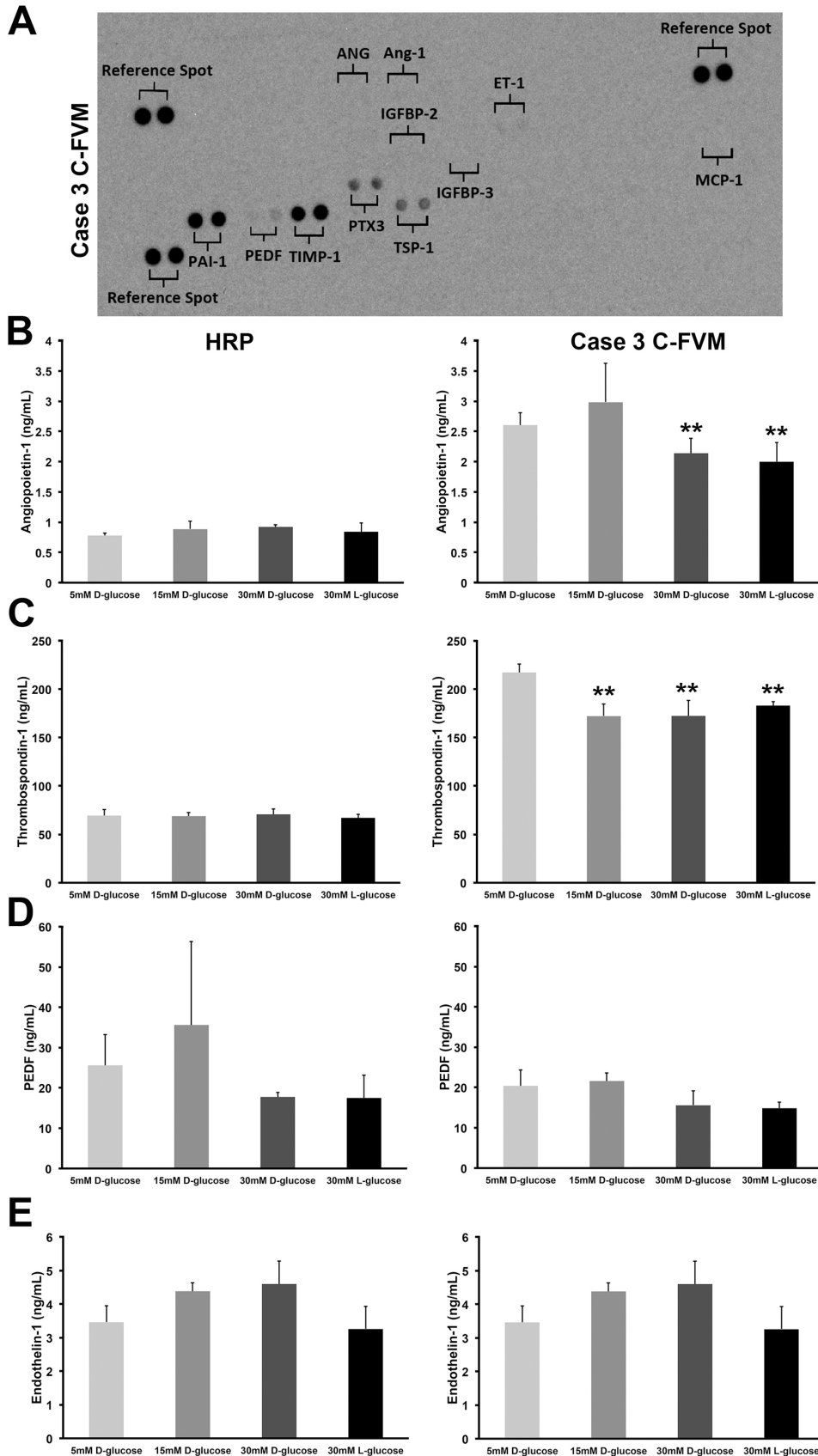
Figure 6. Angiogenesis-related proteins secreted by C-FVMs: The effect of high glucose and hyperosmolarity. Map of the human angiogenesis antibody array targeting 55 proteins related to angiogenesis and angiogenesis-related factors identified 11 proteins secreted by C-FVMs from clinical case 3 (**A**). For identity and coordinates of all 55 proteins assayed, see Appendix 4. Protein levels of (**B**) angiopoietin-1, (**C**) thrombospondin-1, (**D**) PEDF, and (**E**) endothelin-1 under different glucose treatments were measured in human retinal pericytes (HRP) and C-FVMs from clinical case 3 using an ELISA assay. Student *t* tests show there was a significant reduction in levels of angiopoietin-1 and thrombospondin-1 by cells grown in high glucose (30 mM D-glucose) and under hyperosmolar conditions (30 mM L-glucose), as compared to normal glucose and normal osmolar conditions (5 mM). No changes in PEDF or endothelin-1 protein levels were observed in C-FVMs in response to changes in glucose or osmolarity conditions. The levels of angiopoietin-1, thrombospondin-1, PEDF, and endothelin-1 did not in change in HRP in response to treatment with different glucose or osmolar conditions. Error bars represent ± standard deviations; **$p < 0.01$; n=3.

Tsp-1 within the diabetic environment may further contribute to aberrant angiogenesis.

We found no staining for RPE65 in FVMs. This result is in contrast with the suggestion that RPE cells migrate into FVMs or that RPE cells can migrate through retinal holes in combined tractional retinal detachment (TRD)/ rhegmatogenous retinal detachment (RRD) to invest FVMs within these patients [53]. Three out of five patients from whom the FVMs were obtained had concurrent rhegmatogenous retinal detachment, which would presumably provide access for the RPE to the vitreous cavity. The absence of RPE65 staining suggests that, in contrast to the formation of epiretinal membranes in proliferative vitreoretinopathy, differentiated RPE cells may not play a significant role in the formation of the FVM, although we cannot rule out the possibility that RPE cells downregulate RPE65 expression as they undergo epithelial mesenchymal transition (EMT) [54,55]. Surprisingly, we found that bestrophin-1 was expressed in neovessels in all FVM samples evaluated with immunohistochemistry. Although bestrophin-1 in the eye is generally considered a marker of RPE cells, bestrophins have also been shown to be expressed in vascular smooth cells within the mesenteric arteries and function as an important regulator of vascular constriction [56]. The role of bestrophin-1 in neovessels within the setting of PDR has yet to be clarified; however, expression of bestrophin-1 in new vessels of FVMs has not previously been observed.

Ultimately, PDR is a disorder involving the progression of activities including cell migration into the vitreous, cell division, release of angiogenic factors, and generation of tractional forces. Identification of the cellular constituency of FVMs and the ability to establish these cells in culture is a step toward understanding the pathogenesis of late-stage PDR. Because almost 90% of patients with PDR have bilateral disease at their primary examination [57] and because fibrovascular proliferation may relapse over time [58], it is common for patients undergo multiple surgical procedures to remove FVMs, and FVM specimens could be available from the same individual over a period of months to several years. In the future, we believe that the analysis of the cellular and molecular components of FVMs could provide information to allow for the discovery of novel cell signaling mechanisms linked to PDR.

APPENDIX 1. TABLE OF CLINICAL DEMOGRAPHICS AND PATIENT INFORMATION.

CF=counting fingers; CGH=comparative genomic hybridization; DM=diabetes mellitus; Dx=diagnosis; EM=electron microscopy; F=female; FVM=fibrovascular membrane;

M=male; HM=hand motions; IHC=immunohistochemistry; LP=light perception; NA=not available; NV=neovascular; NVI=neovascularization of the iris; NVG=neovascular glaucoma; OD=right eye; OS=left eye; POM3=post-operative month 3; RRD=rhegmatogenous retinal detachment; SNP=single nucleotide polymorphism; TRD=tractional retinal detachment; Va=visual acuity; VH=vitreous hemorrhage. To access the data, click or select the words "Appendix 1."

APPENDIX 2. FVMS CONTAIN VESSELS WITH ABNORMAL VASCULAR MORPHOLOGY.

(**A**, **B**) Electron micrographs illustrate numerous blood vessels and vessel-like structures (*black arrows*), cells within the FVM stroma that are not associated with vascular structures (*white arrows*), as well as large areas of fibrosis (*Fi*) within a FVM resected from clinical case 1. Ultrastructural analysis reveals vessels with varying degrees of vascular abnormalities (**C** and **D**), with multiple intercellular junctions between endothelial cells (*black arrows*), irregular perivascular cell investment (*P*), swollen mitochondria (***), and abnormal plasma membrane infoldings (*white arrowheads*). n=nucleus, *Lu*=Lumen. Scale bars: (**A**, **B**)=10 μm; (**C**, **D**)=2 μm. To access the data, click or select the words "Appendix 2."

APPENDIX 3. TABLE OF COPY NUMBER VARIATIONS OF GENOMIC DNA FROM PAIRED SAMPLES OF FVM AND BLOOD.

Amp=amplification; bps=base pairs; Chr=chromosome; Del=deletion. To access the data, click or select the words "Appendix 3."

APPENDIX 4. TABLE OF IDENTITY AND COORDINATES OF THE 55 PROTEINS IN THE HUMAN ANGIOGENESIS ANTIBODY ARRAY.

To access the data, click or select the words "Appendix 4."

APPENDIX 5. MRNA EXPRESSION LEVELS OF ANGIOGENESIS-RELATED GENES IN C-FVM.

Expression of angiopoietin-1, thrombospondin-1, PEDF, and endothelin-1 was detected in C-FVM from clinical case 3 by RT-qPCR. Error bars represent ± standard deviation. To access the data, click or select the words "Appendix 5."

REFERENCES

1. Cheung N, Mitchell P, Wong TY. Diabetic retinopathy. Lancet 2010; 376:124-36. [PMID: 20580421].

2. Klein R, Klein BE, Moss SE, Davis MD, DeMets DL. The Wisconsin epidemiologic study of diabetic retinopathy. III. Prevalence and risk of diabetic retinopathy when age at diagnosis is 30 or more years. Arch Ophthalmol 1984; 102:527-32. [PMID: 6367725].

3. Yau JW, Rogers SL, Kawasaki R, Lamoureux EL, Kowalski JW, Bek T, Chen SJ, Dekker JM, Fletcher A, Grauslund J, Haffner S, Hamman RF, Ikram MK, Kayama T, Klein BE, Klein R, Krishnaiah S, Mayurasakorn K, O'Hare JP, Orchard TJ, Porta M, Rema M, Roy MS, Sharma T, Shaw J, Taylor H, Tielsch JM, Varma R, Wang JJ, Wang N, West S, Xu L, Yasuda M, Zhang X, Mitchell P, Wong TY. Global prevalence and major risk factors of diabetic retinopathy. Diabetes Care 2012; 35:556-64. [PMID: 22301125].

4. Antonetti DA, Klein R, Gardner TW. Diabetic retinopathy. N Engl J Med 2012; 366:1227-39. [PMID: 22455417].

5. Eliott D, Lee M, Abrams GW. Proliferative diabetic retinopathy: principles and techniques of surgery. In: Ryan SJ, editor. Retina. 4th ed: Elsevier; 2005.

6. Adamis AP, Miller JW, Bernal MT, D'Amico DJ, Folkman J, Yeo TK, Yeo KT. Increased vascular endothelial growth factor levels in the vitreous of eyes with proliferative diabetic retinopathy. Am J Ophthalmol 1994; 118:445-50. [PMID: 7943121].

7. Aiello LP, Avery RL, Arrigg PG, Keyt BA, Jampel HD, Shah ST, Pasquale LR, Thieme H, Iwamoto MA, Park JE, Nguyen HV, Aiello LM, Ferrara N, King GL. Vascular endothelial growth factor in ocular fluid of patients with diabetic retinopathy and other retinal disorders. N Engl J Med 1994; 331:1480-7. [PMID: 7526212].

8. Miller JW, Adamis AP, Aiello LP. Vascular endothelial growth factor in ocular neovascularization and proliferative diabetic retinopathy. Diabetes Metab Rev 1997; 13:37-50. [PMID: 9134347].

9. Joussen AM, Poulaki V, Le ML, Koizumi K, Esser C, Janicki H, Schraermeyer U, Kociok N, Fauser S, Kirchhof B, Kern TS, Adamis AP. A central role for inflammation in the pathogenesis of diabetic retinopathy. FASEB J 2004; 18:1450-2. [PMID: 15231732].

10. Avery RL, Pearlman J, Pieramici DJ, Rabena MD, Castellarin AA, Nasir MA, Giust MJ, Wendel R, Patel A. Intravitreal bevacizumab (Avastin) in the treatment of proliferative diabetic retinopathy. Ophthalmology 2006; 113:1695- [PMID: 17011951].

11. Bakri SJ, Donaldson MJ, Link TP. Rapid regression of disc neovascularization in a patient with proliferative diabetic retinopathy following adjunctive intravitreal bevacizumab. Eye (Lond) 2006; 20:1474-5. [PMID: 16680105].

12. Spaide RF, Fisher YL. Intravitreal bevacizumab (Avastin) treatment of proliferative diabetic retinopathy complicated by vitreous hemorrhage. Retina 2006; 26:275-8. [PMID: 16508426].

13. Arevalo JF, Maia M, Flynn HW Jr, Saravia M, Avery RL, Wu L, Eid Farah M, Pieramici DJ, Berrocal MH, Sanchez JG. Tractional retinal detachment following intravitreal bevacizumab (Avastin) in patients with severe proliferative diabetic retinopathy. Br J Ophthalmol 2008; 92:213-6. [PMID: 17965108].

14. Sohn EH, He S, Kim LA, Salehi-Had H, Javaheri M, Spee C, Dustin L, Hinton DR, Eliott D. Angiofibrotic response to vascular endothelial growth factor inhibition in diabetic retinal detachment: report no. 1. Arch Ophthalmol 2012; 130:1127-34. [PMID: 22965588].

15. Buckley S, Jenkins L, Benjamin L. Field loss after pan retinal photocoagulation with diode and argon lasers. Doc Ophthalmol 1992; 82:317-22. [PMID: 1306479].

16. Engerman RL, Kern TS. Retinopathy in animal models of diabetes. Diabetes Metab Rev 1995; 11:109-20. [PMID: 7555563].

17. Rees DA, Alcolado JC. Animal models of diabetes mellitus. Diabetic Medicine. Journal of the British Diabetic Association 2005; 22:359-70. .

18. Rakoczy EP, Ali Rahman IS, Binz N, Li CR, Vagaja NN, de Pinho M, Lai CM. Characterization of a mouse model of hyperglycemia and retinal neovascularization. Am J Pathol 2010; 177:2659-70. [PMID: 20829433].

19. Jo DH, Cho CS, Kim JH, Jun HO. Animal models of diabetic retinopathy: doors to investigate pathogenesis and potential therapeutics. J Biomed Sci 2013; 20:38-[PMID: 23786217].

20. Hammes HP, Lin J, Renner O, Shani M, Lundqvist A, Betsholtz C, Brownlee M, Deutsch U. Pericytes and the pathogenesis

of diabetic retinopathy. Diabetes 2002; 51:3107-12. [PMID: 12351455].

21. Armulik A, Genove G, Betsholtz C. Pericytes: developmental, physiological, and pathological perspectives, problems, and promises. Dev Cell 2011; 21:193-215. [PMID: 21839917].

22. Enge M, Bjarnegkård M, Gerhardt H, Gustafsson E, Kalen M, Asker N, Hammes HP, Shani M, Fassler R, Betsholtz C. Endothelium-specific platelet-derived growth factor-B ablation mimics diabetic retinopathy. EMBO J 2002; 21:4307-16. [PMID: 12169633].

23. Bjarnegard M, Enge M, Norlin J, Gustafsdottir S, Fredriksson S, Abramsson A, Takemoto M, Gustafsson E, Fassler R, Betsholtz C. Endothelium-specific ablation of PDGFB leads to pericyte loss and glomerular, cardiac and placental abnormalities. Development 2004; 131:1847-57. [PMID: 15084468].

24. Valdez CN, Arboleda-Velasquez JF, Amarnani DS, Kim LA, D'Amore PA. Retinal microangiopathy in a mouse model of inducible mural cell loss. Am J Pathol 2014; 184:2618-26. [PMID: 25092275].

25. Nakao S, Arima M, Ishikawa K, Kohno R, Kawahara S, Miyazaki M, Yoshida S, Enaida H, Hafezi-Moghadam A, Kono T, Ishibashi T. Intravitreal anti-VEGF therapy blocks inflammatory cell infiltration and re-entry into the circulation in retinal angiogenesis. Invest Ophthalmol Vis Sci 2012; 53:4323-8. [PMID: 22661475].

26. Al-Shabrawey M, Mussell R, Kahook K, Tawfik A, Eladl M, Sarthy V, Nussbaum J, El-Marakby A, Park SY, Gurel Z, Sheibani N, Maddipati KR. Increased expression and activity of 12-lipoxygenase in oxygen-induced ischemic retinopathy and proliferative diabetic retinopathy: implications in retinal neovascularization. Diabetes 2011; 60:614-24. [PMID: 21228311].

27. Grossniklaus HE, Kang SJ, Berglin L. Animal models of choroidal and retinal neovascularization. Prog Retin Eye Res 2010; 29:500-19. [PMID: 20488255].

28. Lai AK, Lo AC. Animal models of diabetic retinopathy: summary and comparison. J Diabetes Res 2013; 2013:106594-[PMID: 24286086].

29. Onat D, Brillon D, Colombo PC, Schmidt AM. Human vascular endothelial cells: a model system for studying vascular inflammation in diabetes and atherosclerosis. Curr Diab Rep 2011; 11:193-202. [PMID: 21337131].

30. Tonna S, El-Osta A, Cooper ME, Tikellis C. Metabolic memory and diabetic nephropathy: potential role for epigenetic mechanisms. Nat Rev Nephrol 2010; 6:332-41. [PMID: 20421885].

31. Siebel AL, Fernandez AZ, El-Osta A. Glycemic memory associated epigenetic changes. Biochem Pharmacol 2010; 80:1853-9. [PMID: 20599797].

32. Vereb Z, Lumi X, Andjelic S, Globocnik-Petrovic M, Urbancic M, Hawlina M, Facsko A, Petrovski G. Functional and molecular characterization of ex vivo cultured epiretinal membrane

cells from human proliferative diabetic retinopathy. Biomed Res Int 2013; 2013:492376-[PMID: 24195074].

33. World Medical Association declaration of Helsinki. Recommendations guiding physicians in biomedical research involving human subjects. JAMA 1997; 277:925-6. [PMID: 9062334].

34. Kubota T, Morita H, Tou N, Nitta N, Tawara A, Satoh H, Shimajiri S. Histology of fibrovascular membranes of proliferative diabetic retinopathy after intravitreal injection of bevacizumab. Retina 2010; 30:468-72. [PMID: 19952991].

35. Akino T, Hida K, Hida Y, Tsuchiya K, Freedman D, Muraki C, Ohga N, Matsuda K, Akiyama K, Harabayashi T, Shinohara N, Nonomura K, Klagsbrun M, Shindoh M. Cytogenetic abnormalities of tumor-associated endothelial cells in human malignant tumors. Am J Pathol 2009; 175:2657-67. [PMID: 19875502].

36. Hida K, Klagsbrun M. A new perspective on tumor endothelial cells: unexpected chromosome and centrosome abnormalities. Cancer Res 2005; 65:2507-10. [PMID: 15805239].

37. Hida K, Hida Y, Amin DN, Flint AF, Panigrahy D, Morton CC, Klagsbrun M. Tumor-associated endothelial cells with cytogenetic abnormalities. Cancer Res 2004; 64:8249-55. [PMID: 15548691].

38. Pugh TJ, Delaney AD, Farnoud N, Flibotte S, Griffith M, Li HI, Qian H, Farinha P, Gascoyne RD, Marra MA. Impact of whole genome amplification on analysis of copy number variants. Nucleic Acids Res 2008; 36:e80-[PMID: 18559357].

39. van de Wiel MA, Picard F, van Wieringen WN, Ylstra B. Preprocessing and downstream analysis of microarray DNA copy number profiles. Brief Bioinform 2011; 12:10-21. [PMID: 20172948].

40. Wang Q, Peng P, Qian M, Wan L, Deng M. Hybridization and amplification rate correction for affymetrix SNP arrays. BMC Med Genomics 2012; 5:24-[PMID: 22691279].

41. Antonelli-Orlidge A, Saunders KB, Smith SR, D'Amore PA. An activated form of transforming growth factor beta is produced by cocultures of endothelial cells and pericytes. Proc Natl Acad Sci USA 1989; 86:4544-8. [PMID: 2734305].

42. Armulik A, Abramsson A, Betsholtz C. Endothelial/pericyte interactions. Circ Res 2005; 97:512-23. [PMID: 16166562].

43. Pfister F, Przybyt E, Harmsen MC, Hammes HP. Pericytes in the eye. Pflugers Arch 2013; 465:789-96. [PMID: 23568370].

44. Fong DS, Ferris FL 3rd, Davis MD, Chew EY. Causes of severe visual loss in the early treatment diabetic retinopathy study: ETDRS report no. 24. Early Treatment Diabetic Retinopathy Study Research Group. Am J Ophthalmol 1999; 127:137-41. [PMID: 10030553].

45. Wang S, Wu Z, Sorenson CM, Lawler J, Sheibani N. Thrombospondin-1-deficient mice exhibit increased vascular density during retinal vascular development and are less sensitive to hyperoxia-mediated vessel obliteration. Dev Dyn 2003; 228:630-42. [PMID: 14648840].

46. Thurston G, Suri C, Smith K, McClain J, Sato TN, Yancopoulos GD, McDonald DM. Leakage-resistant blood vessels

in mice transgenically overexpressing angiopoietin-1. Science 1999; 286:2511-4. [PMID: 10617467].

47. Uemura A, Ogawa M, Hirashima M, Fujiwara T, Koyama S, Takagi H, Honda Y, Wiegand SJ, Yancopoulos GD, Nishikawa S. Recombinant angiopoietin-1 restores higher-order architecture of growing blood vessels in mice in the absence of mural cells. J Clin Invest 2002; 110:1619-28. [PMID: 12464667].

48. Cai J, Kehoe O, Smith GM, Hykin P, Boulton ME. The angiopoietin/Tie-2 system regulates pericyte survival and recruitment in diabetic retinopathy. Invest Ophthalmol Vis Sci 2008; 49:2163-71. [PMID: 18436850].

49. Suri C, Jones PF, Patan S, Bartunkova S, Maisonpierre PC, Davis S, Sato TN, Yancopoulos GD. Requisite role of angiopoietin-1, a ligand for the TIE2 receptor, during embryonic angiogenesis. Cell 1996; 87:1171-80. [PMID: 8980224].

50. Kim I, Moon SO, Park SK, Chae SW, Koh GY. Angiopoietin-1 reduces VEGF-stimulated leukocyte adhesion to endothelial cells by reducing ICAM-1, VCAM-1, and E-selectin expression. Circ Res 2001; 89:477-9. [PMID: 11557733].

51. Patel JI, Hykin PG, Gregor ZJ, Boulton M, Cree IA. Angiopoietin concentrations in diabetic retinopathy. Br J Ophthalmol 2005; 89:480-3. [PMID: 15774928].

52. Sheibani N, Frazier WA. Thrombospondin 1 expression in transformed endothelial cells restores a normal phenotype and suppresses their tumorigenesis. Proc Natl Acad Sci USA 1995; 92:6788-92. [PMID: 7624320].

53. Peters MA, Burke JM, Clowry M, Abrams GW, Williams GA. Development of traction retinal detachments following intravitreal injections of retinal Muller and pigment epithelial cells. Graefes Arch Clin Exp Ophthalmol 1986; 224:554-63. [PMID: 3792852].

54. Hatanaka H, Koizumi N, Okumura N, Kay EP, Mizuhara E, Hamuro J, Kinoshita S. Epithelial-mesenchymal transition-like phenotypic changes of retinal pigment epithelium induced by TGF-beta are prevented by PPAR-gamma agonists. Invest Ophthalmol Vis Sci 2012; 53:6955-63. [PMID: 22956604].

55. Chen HC, Zhu YT, Chen SY, Tseng SC. Wnt signaling induces epithelial-mesenchymal transition with proliferation in ARPE-19 cells upon loss of contact inhibition. Lab Invest 2012; 92:676-87. [PMID: 22391957].

56. Broegger T, Jacobsen JC, Secher Dam V, Boedtkjer DM, Kold-Petersen H, Pedersen FS, Aalkjaer C, Matchkov VV. Bestrophin is important for the rhythmic but not the tonic contraction in rat mesenteric small arteries. Cardiovasc Res 2011; 91:685-93. [PMID: 21498420].

57. Valone JA Jr, McMeel JW, Franks EP. Unilateral proliferative diabetic retinopathy. II. Clinical course. Arch Ophthalmol 1981; 99:1362-6. [PMID: 7259606].

58. Hsu YR, Yang CM, Yeh PT. Clinical and histological features of epiretinal membrane after diabetic vitrectomy. Graefes Arch Clin Exp Ophthalmol 2014; 252:401-10. [PMID: 24126678].